Transport and Temperature: Exact Spectrum and Drude Weight for the One-Dimensional Infinite-U Hubbard Model

Shuo Liu,[1] Yuhao Ma,[2] Hitesh J. Changlani,[3,4] Philip W. Phillips,[2] and B. Andrei Bernevig[1,5,6,*]
[1]Department of Physics, Princeton University, Princeton, New Jersey 08544, USA
[2]Department of Physics and Institute of Condensed Matter Theory, University of Illinois at Urbana-Champaign, Urbana, Illinois 61801, USA
[3]National High Magnetic Field Laboratory, Tallahassee, Florida 32310, USA
[4]Department of Physics, Florida State University, Tallahassee, Florida 32306, USA
[5]Donostia International Physics Center (DIPC), Paseo Manuel de Lardizábal, 20018 San Sebastián, Spain
[6]IKERBASQUE, Basque Foundation for Science, 48013 Bilbao, Spain

(Received 29 April 2026; revised 11 August 2026; accepted 9 September 2026; published 14 October 2026)

Understanding charge transport in strongly correlated systems remains a central challenge in condensed matter physics, while exact analytical results for finite-temperature transport remain rare. Here, we investigate charge transport in the one-dimensional Hubbard model in the infinite-interaction limit. We first construct the exact and *explicit*, i.e., *beyond Bethe ansatz* energy spectrum and eigenstates. Building on these explicit eigenstates, we derive a closed-form analytical expression for the charge Drude weight at arbitrary temperatures in the hole-dilute limit with a fixed number of doped holes, as well as analytical expressions in the low- and high-temperature limits at fixed hole density. We further show that, at low temperatures, the leading correction to the charge Drude weight is linear in T when the number of holes is fixed, whereas it is quadratic in T when the hole density is fixed. This analytically controlled example highlights the importance of identifying the underlying thermodynamic trajectory when interpreting finite-size numerical studies of charge transport in more general models.

DOI: 10.1103/2fwz-cw5h

Introduction—Since the experimental discovery of high-temperature superconductivity (SC) in cuprates several decades ago, a consensus on the underlying microscopic mechanism has remained elusive [1–7]. One point of agreement is that the answer lies in the solution to the doped Mott insulator problem [3]. Central to this problem is the dynamical generation of a charge gap in half-filled band [3,8]. In this regard, the two-dimensional (2D) Hubbard model [9–11] is viewed as the gold standard for the copper-oxide layer. Other popular models include the t-J model that approximates the dynamical physics of the Hubbard model. However, these strongly correlated 2D systems remain analytically intractable. Numerical simulations also face severe limitations, such as the limited system widths accessible to density matrix renormalization group [12] or the sign problem in quantum Monte Carlo simulation [13–22]. Additionally, we note recent developments utilizing neural quantum states [23–25].

An extreme limit of the t-J model is the $J = 0$ case in which the high-energy sector is completely decoupled. As J is inversely related to the coupling constant in the Hubbard model, $J = 0$ can be viewed as the infinite-interaction limit [26,27]. Even a single hole in this background is a nontrivial problem and the resultant transport properties remain unknown. For certain classes of lattices (there are now generalizations to honeycomb and diamond lattices [28]), the Nagaoka theorem tells us that a fully polarized ferromagnetic state is the ground state [26]. Counterexamples to the Nagaoka theorem have also been investigated on frustrated lattices, including the 120° antiferromagnetic ground state on the triangular lattice [29–31] and the exact resonating-valence-bond spin-liquid ground state on the checkerboard lattice [32]. Besides these analytical results, a number of intriguing phenomena have been reported in this infinite-interaction limit, based on numerical studies and experiments. These include kinetically induced hole-magnon bound states [33–36] on the triangular lattice and, remarkably, signatures of strange-metal transport on the square lattice with a single doped hole [37]. However, even in this infinite-interaction limit, more general situations such as multiple doped holes remain highly nontrivial and analytically challenging.

A natural starting point for analytically understanding the physics of the 2D Hubbard model [9–11,38–48] is its one-dimensional (1D) counterpart [49]. The 1D Hubbard model is integrable and thus admits an exact solution via the Bethe ansatz [50–57]. Despite this integrability, the Bethe ansatz solutions are not explicit, and a comprehensive analytical understanding of transport remains highly

*Contact author: bernevig@princeton.edu

 © 2026 American Physical Society

nontrivial [58–68]. At half filling, the system is a Mott insulator, and consequently the charge Drude weight vanishes [69–72]. Away from half filling, the charge Drude weight becomes finite [73–79]. Its exact expression at zero temperature has been obtained in Refs. [73,74,80]. The leading finite-temperature correction was later derived from the finite-size corrections to the thermodynamic Bethe ansatz equations, yielding a T^2 dependence [81]. However, the full temperature dependence of the Drude weight remains unknown, and no simple analytical expression has been established. Consequently, much of the existing understanding relies on numerical approaches [82–87].

In this Letter, we focus on the 1D Hubbard model in the infinite-interaction limit. We first construct the exact but more importantly *explicit* eigenstates and energy spectrum of the Hamiltonian [see Sec. III of Supplemental Material (SM) [88]]. Our systematic construction in the occupation basis captures the nontrivial spin-sector degeneracies and corresponding boundary twists. Building on these explicit eigenstates, we then derive an analytical expression for the charge Drude weight at arbitrary temperatures with a single doped hole (see Sec. IV of SM [88]), whose form becomes particularly simple in the large-system-size limit [see Eq. (15)]. The result can be straightforwardly generalized to an arbitrary but finite number of doped holes (see Sec. IV of SM [88]). In this hole-dilute limit, where the number of holes n_h is kept fixed as the large-system-size limit is taken, the charge carriers propagate essentially independently. Consequently, n_h enters as an overall prefactor in the Drude weight. Furthermore, for a fixed density δ of doped holes, where $\delta = n_h/N$ is fixed in the thermodynamic limit $N \to \infty$, we derive analytical expressions for the charge Drude weight in both the low- and high-temperature limits (see Sec. V of SM [88]). We note that these explicit eigenstates may also provide insight into other properties of the present model, including spin transport [61,68].

More importantly, based on the analytical expression, we further analyze the low-temperature scaling of the charge Drude weight for both a single doped hole and a fixed density of holes, as summarized in Table I. We find that the leading temperature dependence of the Drude weight is linear in T for a single doped hole, whereas it exhibits a T^2 correction at a fixed hole density. The latter scaling is consistent with the results in Ref. [81]; moreover, our calculation provides the exact analytical expression for the corresponding expansion coefficient.

The linear-in-T resistivity behaviors associated with strange-metal phenomenology have been reported in numerical studies of the 2D Hubbard model [37,100–104] and in experiments on cuprate superconductors at fixed doping [105–116]. We also note that Sachdev-Ye-Kitaev-type models can produce linear-in-T resistivity in the all-to-all interaction configuration [117–120], and similar behavior has also been observed in twisted bilayer graphene [121–124]. Although the present 1D infinite-U Hubbard model is neither equivalent to the 2D Hubbard model nor a realistic microscopic description of cuprate materials, it provides an analytically controlled example demonstrating that the fixed-hole-number and fixed-hole-density thermodynamic limits can exhibit qualitatively distinct charge-transport behaviors. Therefore, extreme caution is required when extrapolating 2D finite-size numerical results—especially those from exact diagonalization (ED)—to finite-doping strange-metal phenomenology (see Sec. VI of SM [88] for further details, including a discussion of the respective limitations of ED, quantum Monte Carlo, and density matrix renormalization group). In such ED calculations, severely restricted cluster sizes often inherently constrain the system to a fixed-carrier-number trajectory rather than a true fixed-density limit. This limitation further underscores the need for analytical solutions.

Model and definition of optical conductivity—In this Letter, we consider the 1D Hubbard model in the infinite-interaction limit. The Hamiltonian is given by

$$\hat{H} = -t \sum_{\sigma=\{\uparrow,\downarrow\}} \sum_{j=0}^{N-1} \left(\tilde{c}^{\dagger}_{j+1,\sigma} \tilde{c}_{j,\sigma} + \tilde{c}^{\dagger}_{j,\sigma} \tilde{c}_{j+1,\sigma} \right), \quad (1)$$

where $\tilde{c}^{\dagger}_{j,\sigma} = (1 - n_{j,\bar{\sigma}}) c^{\dagger}_{j,\sigma}$ denotes the projected creation operator for a fermion with spin σ at site j and $n_{j,\bar{\sigma}} = c^{\dagger}_{j,\bar{\sigma}} c_{j,\bar{\sigma}}$ is the density operator for fermions with the opposite spin $\bar{\sigma}$, thereby enforcing the no-double-occupancy constraint that encodes the strong-correlation physics of the infinite-U limit and distinguishes the model from a noninteracting system. The hopping amplitude t sets the overall energy scale, and we set $t = 1$ throughout this Letter. We impose periodic boundary conditions, such that $\tilde{c}^{\dagger}_{N,\sigma} \equiv \tilde{c}^{\dagger}_{0,\sigma}$, where N is the total number of lattice sites. Moreover, we denote by n_h the number of doped holes in the system.

TABLE I. Analytical expressions for the charge Drude weight in different limits.

Case	High-temperature limit	Low-temperature limit
Single hole	$D_{1h}(T \to \infty) = (1/NT)$	$D_{1h}(T \to 0) = (1/N)(1 - T/4)$
Fixed number of holes n_h	$D_{n_h}(T \to \infty) = (n_h/NT)$	$D_{n_h}(T \to 0) = (n_h/N)(1 - T/4)$
Fixed hole density $\delta = n_h/N$	$D_{\delta}(T \to \infty) = [\delta(1-\delta)]/T$	$D_{\delta}(T \to 0) = [\sin(\pi\delta)/\pi] - (\pi T^2/[24\sin(\pi\delta)])$

The real part of the optical conductivity (see Sec. I of SM [88]) can be expressed as

$$\mathrm{Re}\,\sigma(\omega,T)=2\pi D(T)\delta(\omega)+\sigma_{\mathrm{reg}}(\omega,T), \tag{2}$$

where T is the temperature, ω the frequency, $\delta(\cdot)$ the Dirac delta function, $D(T)$ the temperature-dependent charge Drude weight corresponding to the singular contribution at zero frequency, and $\sigma_{\mathrm{reg}}(\omega,T)$ the regular (finite-frequency) contribution. Here, "regular" indicates that this part does not contain a $\delta(\omega)$ singularity at zero frequency. The dc conductivity at zero frequency can be formally decomposed as

$$\sigma_{\mathrm{dc}}(T)=2\pi D(T)\delta(\omega)+\lim_{\omega\to 0}\sigma_{\mathrm{reg}}(\omega,T), \tag{3}$$

consisting of both the Drude weight contribution and the contribution obtained by extrapolating the regular part to $\omega=0$. Note that although $\delta(\omega)$ is singular at $\omega=0$ and has no ordinary pointwise value, we formally retain $\delta(\omega)$ to denote the zero-frequency Drude contribution; the physically meaningful quantity characterizing its spectral weight is the Drude weight $D(T)$. As a consequence, a nonzero Drude weight implies an ideal conductor. Whether the Drude weight is nonzero rests on the existence of conservation laws, as can be seen from the Mazur inequality [78,125],

$$D\geq\frac{\beta}{2N}\sum_{n}\frac{\langle\hat{J}\hat{Q}_n\rangle^2}{\langle\hat{Q}_n^2\rangle}, \tag{4}$$

where $\hat{Q}_n$ is conserved. In typical notation [78], $\hat{Q}_2$ is the Hamiltonian. We find that $\hat{J}$ commutes with the Hamiltonian, implying a nonzero overlap on the rhs of Eq. (4) and hence a finite Drude weight (see Sec. I of SM [88]).

$D(T)$ and $\sigma_{\mathrm{reg}}(\omega,T)$ (see Refs. [73,87,126–129] or Sec. I of SM [88] for a detailed derivation) are given by

$$D(T)=\frac{1}{N}\left[\frac{1}{2}\langle-\hat{K}\rangle-\frac{1}{Z}\sum_{\substack{m,n\\E_m\neq E_n}}e^{-\beta E_n}\frac{|J_{mn}|^2}{E_m-E_n}\right], \tag{5}$$

$$\sigma_{\mathrm{reg}}(\omega,T)=\pi\frac{1-e^{-\beta\omega}}{\omega ZN}\sum_{n,m}e^{-\beta E_n}|J_{mn}|^2\delta(E_n+\omega-E_m), \tag{6}$$

respectively. In Eq. (5) the first term is the diamagnetic response whereas the latter term is the paramagnetic contribution, both of which enter the dc response. Since the paramagnetic contribution is nonnegative, the diamagnetic response provides an upper bound on the Drude weight (see Sec. I of SM [88]). Note that the expression for the regular part in Eq. (6) does not apply strictly at zero frequency, as is clear from the derivation presented in Sec. I [88]. Here $\beta=1/T$ is the inverse temperature, $\hat{K}$ denotes the kinetic-energy operator, which coincides with the Hamiltonian $\hat{H}$ in the present model (see Sec. I of SM [88]), and $\langle-\hat{K}\rangle=\mathrm{Tr}(-\hat{K}e^{-\beta\hat{H}})/Z$ denotes its thermal expectation value, where $Z=\mathrm{Tr}(e^{-\beta\hat{H}})$ is the partition function, E_n is the eigenenergy of the n th eigenstate $|n\rangle$ of the Hamiltonian $\hat{H}$. The charge current operator $\hat{J}$ (see Sec. II of SM [88]) is

$$\hat{J}=i\sum_{\sigma=\{\uparrow,\downarrow\}}\sum_{j=0}^{N-1}\left(\tilde{c}^{\dagger}_{j+1,\sigma}\tilde{c}_{j,\sigma}-\tilde{c}^{\dagger}_{j,\sigma}\tilde{c}_{j+1,\sigma}\right), \tag{7}$$

and its matrix elements in the eigenbasis of $\hat{H}$ are defined as $J_{mn}=\langle m|\hat{J}|n\rangle$.

Exact solutions of the energy spectrum—Inspired by the frozen-spin structure, namely, the fact that the action of $\hat{H}$ preserves the relative cyclic ordering of the spin-up and spin-down fermions, we have obtained the complete set of eigenstates and the energy spectrum explicitly. The detailed derivations, including the explicit expressions for the eigenstates for the cases with one hole, two holes, and an arbitrary number of holes, are presented in Sec. III [88]. Below, we present only the energy spectrum with a single doped hole.

In the fully polarized sector with $S_z=\frac{1}{2}\sum_j(n_{j,\uparrow}-n_{j,\downarrow})=\pm(N-1)/2$, corresponding to $N-1$ spin-up fermions (or $N-1$ spin-down fermions), the energy spectrum (see Sec. III [88]) is

$$E(m)=2\cos\left(\frac{2\pi m}{N}\right), \tag{8}$$

where $m=0,\ldots,N-1$ labels the distinct eigenstates.

More generally, in the sector with $S_z=(N-1)/2-n_{\downarrow}$ and $0<n_{\downarrow}<N-1$, where $n_{\downarrow}$ denotes the number of spin-down fermions, the energy levels take the form (see Sec. III of SM [88])

$$E(m,m_{\downarrow})=2\cos\left(\frac{2\pi m}{N}+\frac{2\pi m_{\downarrow}}{N(N-1)}\right), \tag{9}$$

with $m=0,\ldots,N-1$ and $m_{\downarrow}=0,\ldots,N-2$. The degeneracy of each such energy level is $1/(N-1)\binom{N-1}{n_{\downarrow}}$. For finite-size systems, additional eigenvalues not captured by Eq. (9) may appear. However, as discussed in Sec. III [88], the number of such states is negligible in the thermodynamic limit and therefore does not affect the analytical results for charge transport presented below.

We note that Eqs. (8) and (9) are consistent with the spin-charge separation exhibited in the present model [57]: its charge degrees of freedom can be mapped onto noninteracting spinless fermions. However, the spin degrees of freedom affect the spectrum by effectively introducing

twisted boundary conditions, as shown in Eq. (9) and Sec. III of SM [88]; determining these boundary twists explicitly is nontrivial. Moreover, because the explicit many-body eigenstates retain the full information about both the charge and spin degrees of freedom beyond that captured by the noninteracting spinless-fermion model, they may also provide insight into other properties, such as spin transport [61,68].

Analytical expression for the Drude weight—In this section, we present the analytical expression for the Drude weight building upon the explicit energy spectrum and eigenstates. We focus on the case of a single doped hole, and also discuss the cases of an arbitrary fixed number of holes and of a fixed density of holes.

First, we note that in the present model the current operator $\hat{J}$ commutes with the Hamiltonian $\hat{H}$, i.e., $[\hat{J},\hat{H}]=0$ (see Sec. II of SM [88]). By Eq. (4), the Drude weight must be finite. This property is special to the infinite-interaction limit and does not hold for the 1D Hubbard model with finite interaction strength, where generally $[\hat{J},\hat{H}]\neq 0$. As a consequence, $\hat{H}$ and $\hat{J}$ share a common set of eigenstates $|n\rangle$, and thus we have

$$|J_{mn}|=0 \text{ when } m\neq n, \tag{10}$$

which is also true for degenerate states (see Sec. II of SM [88]). Together with $\hat{K}=\hat{H}$ for the present model, the Drude weight in Eq. (5) simplifies to

$$D(T)=\frac{1}{2N}\langle -\hat{H}\rangle, \tag{11}$$

and the regular part in Eq. (6) becomes

$$\sigma_{\mathrm{reg}}(\omega,T)=\pi\frac{1-e^{-\beta\omega}}{\omega ZN}\sum_n e^{-\beta E_n}|J_{nn}|^2\delta(\omega). \tag{12}$$

Therefore, $\sigma_{\mathrm{reg}}(\omega,T)$ vanishes at any nonzero frequency and thus $\lim_{\omega\to 0}\sigma_{\mathrm{reg}}(\omega,T)=0$. Consequently, according to Eq. (3), only the Drude weight shown in Eq. (11) contributes to the dc conductivity for the present model.

Moreover, although Eq. (12) is not directly applicable at strictly zero frequency, taking the $\omega\to 0$ limit of its prefactor, i.e., $\lim_{\omega\to 0}(1-e^{-\beta\omega})/\omega=\beta$, and dividing by 2π yields

$$D_{\mathrm{diff}}(T)=\frac{\beta}{2ZN}\sum_n e^{-\beta E_n}|J_{nn}|^2. \tag{13}$$

It is related to the Drude weight through

$$D_{\mathrm{diff}}(T)=D(T)-D_m(T), \tag{14}$$

that is, it measures the difference between the Drude weight and the Meissner stiffness $D_m(T)$ [130,131]. In Sec. IV [88], we have proven that $D_{\mathrm{diff}}(T)=D(T)$, i.e., $D_m(T)=0$, consistent with the absence of SC in one dimension. Furthermore, because $\hat{J}$ in Eq. (7) is itself conserved, it can be chosen as a conserved charge in the Mazur inequality [see Eq. (4)], which provides a lower bound on the Drude weight [125]. With this choice, the Mazur bound reproduces Eq. (13). Therefore, for the present model, the Mazur lower bound coincides with the exact charge Drude weight.

In the sector with a single doped hole, the analytical expression for the Drude weight in the large-system-size limit reads (see Sec. IV of SM [88])

$$D_{1h}(T)=\frac{\beta}{N}\left(1-\frac{I_2(2\beta)}{I_0(2\beta)}\right), \tag{15}$$

where $I_l(\cdot)$ denotes the l th modified Bessel function of the first kind, arising from the $\cos(\cdot)$ energy spectrum shown in Eqs. (8) and (9). We note that Eq. (15) is the same as that of the noninteracting spinless fermion model due to the spin-charge separation [57]. For a fixed number of doped holes n_h, in the thermodynamic limit, the Drude weight generalizes straightforwardly by acquiring an overall multiplicative factor of n_h (see Sec. IV of SM [88]), reflecting the fact that, in the hole-dilute limit, the holes propagate essentially independently. Beyond this limit, this does not apply. The analytical expressions obtained for the specific heat in Sec. IV [88] also support this point. In the thermodynamic limit, the hole density n_h/N vanishes, and consequently the Drude weight also vanishes, consistent with the Mott-insulating nature of the system at half filling [69–72].

At finite doping with fixed δ, although we do not obtain an analytical expression for the Drude weight $D_\delta(T)$ at arbitrary temperatures, we derive analytical expressions for the Drude weight in both the low- and high-temperature limits (see Sec. V of SM [88]). The analytical expressions for the Drude weight for a fixed number of holes n_h and for a fixed hole density δ in the high- and low-temperature limits are summarized in Table I.

As shown in Table I, at zero temperature, $D_{1h}(T=0)=(1/N)$ and $D_\delta(T=0)=[\sin(\pi\delta)/\pi]$, both of which are consistent with the Luttinger-liquid prediction (Kv_s/π), where $K=1/2$ is the Luttinger parameter for the present model [132,133], and $v_s=[d\varepsilon(k)/dk]|_{k=k_F}=2\sin(\pi\delta)$ is the sound velocity. Note that with fixed n_h, the Fermi momentum scales as $k_F\sim n_h/N$, and the corresponding Fermi energy behaves as $E_F\sim k_F^2\sim n_h^2/N^2$. Therefore, the Luttinger-liquid description, which is valid as a low-energy effective theory only for $T\ll E_F$, applies strictly only at zero temperature.

Temperature scaling of the Drude weight—As summarized in Table I, in the high-temperature limit, the Drude weight scales as $D(T)\propto 1/T$, irrespective of whether the number or density of holes is held fixed. Previous studies of the Hubbard model have reported robust high-temperature scaling of charge-transport quantities [134,135]. More

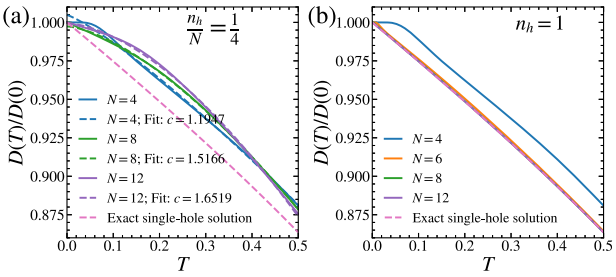


FIG. 1. Normalized Drude weight $D(T)/D(0)$ as a function of temperature T for (a) fixed density of holes $\delta = n_h/N = 1/4$ and (b) a single doped hole. In panel (b), the numerical Drude weight rapidly converges to the analytical prediction as the system size increases. In panel (a), a clearly distinct scaling behavior is observed. By fitting the data to the form $a + bT^c$, we find that the extracted exponent c is larger than 1 and approaches 2 as the system size increases.

interestingly, at low temperatures as shown in Table I, the single-hole Drude weight $D_{1h}(T)$ exhibits a linear-in-T dependence, whereas $D_\delta(T)$ exhibits a quadratic-in-T dependence [81]. This qualitative distinction calls for caution when extrapolating conclusions from finite-size numerical calculations. This issue is particularly relevant to small-cluster ED studies in 2D, for which severe restrictions on accessible system sizes make the finite-density thermodynamic limit difficult to reach.

We have numerically verified these two distinct scaling behaviors using ED. To compare different system sizes, we normalize the Drude weight by its zero-temperature value, i.e., $D(T)/D(0)$. The results are shown in Fig. 1. In Fig. 1(b), corresponding to a single doped hole, the Drude weight obtained from ED rapidly approaches the analytical prediction [Eq. (15)] as the system size increases. In Fig. 1(a), where the density of holes is fixed at $\delta = n_h/N = 1/4$, a direct observation of the quadratic correction is limited by the exponential growth of the Hilbert space. Instead, we fit the numerical data using the form $a + bT^c$ and find that the extracted exponent c approaches the predicted value of 2 as the system size increases. Therefore, the two ways of taking the limit do not commute. As explained in Sec. IV [88], for a fixed number of holes, the system remains in the hole-dilute, nondegenerate regime, where the low-energy excitations are controlled by the quadratic dispersion near the band minimum. As a result, thermal averaging produces a linear-in-T correction to the Drude weight. By contrast, at fixed hole density, the system enters a degenerate Fermi-gas regime, in which the low-energy excitations are governed by the linearized dispersion near the Fermi points. In this case, the Sommerfeld expansion applies and yields the standard T^2 correction to the Drude weight.

Discussion and outlook—In conclusion, we have obtained the explicit energy spectrum and eigenstates (see Sec. III of SM [88]) of the one-dimensional Hubbard model in the infinite-interaction limit and derived a closed-form analytical expression for the charge Drude weight in the hole-dilute regime at arbitrary temperatures, as well as analytical expressions for the Drude weight at finite doping in both the low- and high-temperature limits (see Secs. IV and V [88]). The Drude weight we find is consistent with the Mazur bound [Eq. (4)]. At low temperatures, the leading correction to the Drude weight is linear in T at infinitesimal hole concentration, whereas it is quadratic in T at a fixed finite hole density. Nevertheless, both limits exhibit the same high-temperature scaling.

The distinct temperature scalings of the Drude weight revealed by our analytically controlled example highlight the importance of identifying the underlying thermodynamic trajectory when interpreting finite-size numerical studies of charge transport in more general models. In a finite system, the Dirac delta functions associated with both the Drude and regular contributions in Eq. (2) should be broadened to obtain a smooth conductivity. Consequently, linear-in-T and quadratic-in-T corrections to the Drude weight give rise to corresponding leading temperature corrections to the regularized effective resistivity, as discussed in Sec. VI of SM [88]. This observation underscores the need to distinguish between fixed-carrier-number and fixed-carrier-density thermodynamic trajectories before relating transport scaling obtained from finite-size calculations to finite-doping phenomena, such as the linear-in-T resistivity associated with strange-metal behavior [105–116].

Although the present 1D model is neither equivalent to the 2D Hubbard model, in which signatures of strange-metal transport have been reported numerically [37,100–104], nor a realistic microscopic description of cuprate materials, where such behavior has been observed experimentally [105–116], an interesting direction for future work is to develop perturbative frameworks built on the exact 1D solutions, with the goal of gaining analytical insight into strange-metal transport. For example, a vanishing Drude weight requires the overlap on the rhs of Eq. (4) to vanish. Consequently, it is the lack of conservation of the current that must be at the heart of T-linear resistivity in strongly interacting models. As a result, expansions around the conservation limit are a promising route to strange metallicity. Another promising direction is to seek exact solutions directly in the 2D Hubbard model [136] or in the recently developed momentum-mixing variant of the Hatsugai-Kohmoto model [137,138], for which combined numerical and analytical approaches remain feasible, and then to extract analytical insight from such solutions.

Acknowledgments—We thank Aman Kumar for discussions on a different collaboration. S. L. and B. A. B. were supported by the Gordon and Betty Moore Foundation through Grant No. GBMF8685 toward the Princeton theory program, the Gordon and Betty Moore Foundation's EPiQS Initiative (Grant No. GBMF11070), the Global

Collaborative Network Grant at Princeton University, the Simons Investigator Grant No. 404513, the Princeton Global Network, the NSF MRSEC (Grant No. DMR-2011750), the Simons Collaboration on New Frontiers in Superconductivity (Grants No. SFI-MPS-NFS-00006741-01 and No. SFI-MPS-NFS-00006741-06), the Princeton Catalysis Initiative, the Schmidt Foundation at the Princeton University, European Research Council (ERC) under the European Union's Horizon 2020 research and innovation program (Grant Agreement No. 101020833), the National Science Foundation through the AI Research Institutes program Award No. DMR-2433348. H. J. C. acknowledges funding from National Science Foundation Grant No. DMR 2046570 and the National High Magnetic Field Laboratory (NHMFL). NHMFL is supported by the National Science Foundation through DMR-2128556 and the state of Florida. Y. M. and P. W. P. acknowledge funding from UIUC Research Board, Award No. RB26125.

Data availability—There are no publicly available research data or software supporting this manuscript. Requests for further information or data should be sent to the authors.

[1] E. Dagotto, Correlated electrons in high-temperature superconductors, Rev. Mod. Phys. **66**, 763 (1994).
[2] A. Damascelli, Z. Hussain, and Z.-X. Shen, Angle-resolved photoemission studies of the cuprate superconductors, Rev. Mod. Phys. **75**, 473 (2003).
[3] P. Phillips, Colloquium: Identifying the propagating charge modes in doped Mott insulators, Rev. Mod. Phys. **82**, 1719 (C) (2010).
[4] J. C. S. Davis and D.-H. Lee, Concepts relating magnetic interactions, intertwined electronic orders, and strongly correlated superconductivity, Proc. Natl. Acad. Sci. U.S.A. **110**, 17623 (2013).
[5] E. Fradkin, S. A. Kivelson, and J. M. Tranquada, Colloquium: Theory of intertwined orders in high temperature superconductors, Rev. Mod. Phys. **87**, 457(C) (2015).
[6] B. Keimer, S. A. Kivelson, M. R. Norman, S. Uchida, and J. Zaanen, From quantum matter to high-temperature superconductivity in copper oxides, Nature (London) **518**, 179 (2015).
[7] C. L. Kane, P. A. Lee, and N. Read, Motion of a single hole in a quantum antiferromagnet, Phys. Rev. B **39**, 6880 (1989).
[8] M. B. J. Meinders, H. Eskes, and G. A. Sawatzky, Spectral-weight transfer: Breakdown of low-energy-scale sum rules in correlated systems, Phys. Rev. B **48**, 3916 (1993).
[9] P. W. Anderson, The resonating valence bond state in La_2CuO_4 and superconductivity, Science **235**, 1196 (1987).
[10] F. C. Zhang and T. M. Rice, Effective Hamiltonian for the superconducting Cu oxides, Phys. Rev. B **37**, 3759 (1988).
[11] M. Qin, T. Schäfer, S. Andergassen, P. Corboz, and E. Gull, The Hubbard model: A computational perspective, Annu. Rev. Condens. Matter Phys. **13**, 275 (2022).
[12] E. Stoudenmire and S. R. White, Studying two-dimensional systems with the density matrix renormalization group, Annu. Rev. Condens. Matter Phys. **3**, 111 (2012).
[13] E. Y. Loh, J. E. Gubernatis, R. T. Scalettar, S. R. White, D. J. Scalapino, and R. L. Sugar, Sign problem in the numerical simulation of many-electron systems, Phys. Rev. B **41**, 9301 (1990).
[14] M. Troyer and U.-J. Wiese, Computational complexity and fundamental limitations to fermionic quantum Monte Carlo simulations, Phys. Rev. Lett. **94**, 170201 (2005).
[15] C. Wu and S.-C. Zhang, Sufficient condition for absence of the sign problem in the fermionic quantum Monte Carlo algorithm, Phys. Rev. B **71**, 155115 (2005).
[16] Z.-X. Li, Y.-F. Jiang, and H. Yao, Solving the fermion sign problem in quantum Monte Carlo simulations by Majorana representation, Phys. Rev. B **91**, 241117(R) (2015).
[17] Z.-X. Li, Y.-F. Jiang, and H. Yao, Majorana-time-reversal symmetries: A fundamental principle for sign-problem-free quantum Monte Carlo simulations, Phys. Rev. Lett. **117**, 267002 (2016).
[18] Z. C. Wei, C. Wu, Y. Li, S. Zhang, and T. Xiang, Majorana positivity and the fermion sign problem of quantum Monte Carlo simulations, Phys. Rev. Lett. **116**, 250601 (2016).
[19] Z.-X. Li and H. Yao, Sign-problem-free fermionic quantum Monte Carlo: Developments and applications, Annu. Rev. Condens. Matter Phys. **10**, 337 (2019).
[20] Z.-Q. Wan, S.-X. Zhang, and H. Yao, Mitigating the fermion sign problem by automatic differentiation, Phys. Rev. B **106**, L241109 (2022).
[21] A. J. Kim, P. Werner, and R. Valentí, Alleviating the sign problem in quantum Monte Carlo simulations of spin-orbit-coupled multiorbital Hubbard models, Phys. Rev. B **101**, 045108 (2020).
[22] Y.-F. Song, Y. Deng, and Y.-Y. He, Extended metal-insulator crossover with strong antiferromagnetic spin correlation in half-filled 3D Hubbard model, Phys. Rev. Lett. **134**, 016503 (2025).
[23] C. Roth, A. Chen, A. Sengupta, and A. Georges, Superconductivity in the two-dimensional Hubbard model revealed by neural quantum states, arXiv:2511.07566.
[24] A. Chen, Z.-Q. Wan, A. Sengupta, A. Georges, and C. Roth, Neural network-augmented Pfaffian wave-functions for scalable simulations of interacting fermions, Proc. Natl. Acad. Sci. U.S.A. **123**, 18341e2535288123 (2026).
[25] Y. Gu, W. Li, H. Lin, B. Zhan, R. Li, Y. Huang, D. He, Y. Wu, T. Xiang, M. Qin, L. Wang, and D. Lv, Solving the Hubbard model with neural quantum states, Nat. Commun. **17**, 7838 (2026).
[26] Y. Nagaoka, Ferromagnetism in a narrow, almost half-filled *s* band, Phys. Rev. **147**, 392 (1966).
[27] L. Liu, H. Yao, E. Berg, S. R. White, and S. A. Kivelson, Phases of the infinite *U* Hubbard model on square lattices, Phys. Rev. Lett. **108**, 126406 (2012).
[28] E. Bobrow, K. Stubis, and Y. Li, Exact results on itinerant ferromagnetism and the 15-puzzle problem, Phys. Rev. B **98**, 180101(R) (2018).
[29] J. O. Haerter and B. S. Shastry, Kinetic antiferromagnetism in the triangular lattice, Phys. Rev. Lett. **95**, 087202 (2005).

[30] S. Sherif, P. Sharma, A. Kumar, and H. J. Changlani, Haerter-Shastry kinetic magnetism and metallicity in the triangular Hubbard model, Commun. Phys. **9**, 318 (2026).
[31] P. Sharma, Y. Peng, D. N. Sheng, H. J. Changlani, and Y. Wang, Instability of Nagaoka state and quantum phase transition via kinetic frustration control, Phys. Rev. Res. **8**, 023070 (2026).
[32] C. Glittum, A. Štrkalj, D. Prabhakaran, P. A. Goddard, C. D. Batista, and C. Castelnovo, A resonant valence bond spin liquid in the dilute limit of doped frustrated Mott insulators, Nat. Phys. **21**, 1211 (2025).
[33] S.-S. Zhang, W. Zhu, and C. D. Batista, Pairing from strong repulsion in triangular lattice Hubbard model, Phys. Rev. B **97**, 140507(R) (2018).
[34] I. Morera, A. Bohrdt, W. W. Ho, and E. Demler, Attraction from kinetic frustration in ladder systems, Phys. Rev. Res. **6**, 023196 (2024).
[35] I. M. Navarro, C. Weitenberg, K. Sengstock, and E. Demler, Exploring kinetically induced bound states in triangular lattices with ultracold atoms: Spectroscopic approach, SciPost Phys. **16**, 081 (2024).
[36] M. Qiao, R. Martin, L. Homeier, I. Morera, B. Gély, L. Klein, Y. T. Chew, D. Barredo, T. Lahaye, E. Demler, and A. Browaeys, Kinetically-induced bound states in a frustrated Rydberg tweezer array, arXiv:2510.17183.
[37] S. Fratini, I. Duchemin, A. Ralko, and S. Ciuchi, Strange metal behaviour from underlying bad metallicity, Nat. Phys. (2026).
[38] B. Xiao, Y.-Y. He, A. Georges, and S. Zhang, Temperature dependence of spin and charge orders in the doped two-dimensional Hubbard model, Phys. Rev. X **13**, 011007 (2023).
[39] E. Perepelitsky, A. Galatas, J. Mravlje, R. Žitko, E. Khatami, B. S. Shastry, and A. Georges, Transport and optical conductivity in the Hubbard model: A high-temperature expansion perspective, Phys. Rev. B **94**, 235115 (2016).
[40] D. P. Arovas, E. Berg, S. A. Kivelson, and S. Raghu, The Hubbard model, Annu. Rev. Condens. Matter Phys. **13**, 239 (2022).
[41] E. Gull, O. Parcollet, and A. J. Millis, Superconductivity and the pseudogap in the two-dimensional Hubbard model, Phys. Rev. Lett. **110**, 216405 (2013).
[42] P. Werner and A. J. Millis, Doping-driven Mott transition in the one-band Hubbard model, Phys. Rev. B **75**, 085108 (2007).
[43] E. Gull, M. Ferrero, O. Parcollet, A. Georges, and A. J. Millis, Momentum-space anisotropy and pseudogaps: A comparative cluster dynamical mean-field analysis of the doping-driven metal-insulator transition in the two-dimensional Hubbard model, Phys. Rev. B **82**, 155101 (2010).
[44] R. Valentí and C. Gros, Luttinger liquid instability of the 2D t-J model: A variational study, Phys. Rev. Lett. **68**, 2402 (1992).
[45] M. Schüler, E. G. C. P. van Loon, M. I. Katsnelson, and T. O. Wehling, Thermodynamics of the metal-insulator transition in the extended Hubbard model, SciPost Phys. **6**, 067 (2019).
[46] M. Lu, Y.-F. Song, Y. Deng, and Y.-Y. He, Thermal signatures of the Slater-Mott crossover in the Hubbard model: From double occupancy to antiferromagnetic correlation length, arXiv:2606.10976.
[47] Y.-F. Song, Y. Deng, and Y.-Y. He, Computation of thermal entropy for the doped Hubbard model, Phys. Rev. B **114**, 115101 (2026).
[48] A. Wietek, Y.-Y. He, S. R. White, A. Georges, and E. M. Stoudenmire, Stripes, antiferromagnetism, and the pseudogap in the doped Hubbard model at finite temperature, Phys. Rev. X **11**, 031007 (2021).
[49] F. H. Essler, H. Frahm, F. Göhmann, A. Klümper, and V. E. Korepin, *The One-Dimensional Hubbard Model* (Cambridge University Press, Cambridge, England, 2005).
[50] E. H. Lieb and F. Y. Wu, Absence of Mott transition in an exact solution of the short-range, one-band model in one dimension, Phys. Rev. Lett. **20**, 1445 (1968).
[51] B. S. Shastry, Infinite conservation laws in the one-dimensional Hubbard model, Phys. Rev. Lett. **56**, 1529 (1986).
[52] M. Takahashi, One-dimensional Hubbard model at finite temperature, Prog. Theor. Phys. **47**, 69 (1972).
[53] M. Takahashi, Low-temperature specific-heat of one-dimensional Hubbard model, Prog. Theor. Phys. **52**, 103 (1974).
[54] F. Göhmann and S. Murakami, Fermionic representations of integrable lattice systems, J. Phys. A **31**, 7729 (1998).
[55] A. Izergin, A. Pronko, and N. Abarenkova, Temperature correlators in the one-dimensional Hubbard model in the strong coupling limit, Phys. Lett. A **245**, 537 (1998).
[56] Z. Maassarani and P. Mathieu, The su (N) XX model, Nucl. Phys. **B517**, 395 (1998).
[57] M. Ogata and H. Shiba, Bethe-ansatz wave function, momentum distribution, and spin correlation in the one-dimensional strongly correlated Hubbard model, Phys. Rev. B **41**, 2326 (1990).
[58] X. Zotos, Issues on the transport of one dimensional quantum systems, J. Phys. Soc. Jpn. **74**, 173 (2005).
[59] F. Heidrich-Meisner, A. Honecker, and W. Brenig, Transport in quasi one-dimensional spin-1/2 systems, Eur. Phys. J. Special Topics **151**, 135 (2007).
[60] B. Bertini, F. Heidrich-Meisner, C. Karrasch, T. Prosen, R. Steinigeweg, and M. Žnidarič, Finite-temperature transport in one-dimensional quantum lattice models, Rev. Mod. Phys. **93**, 025003 (2021).
[61] O. Gamayun, A. Hutsalyuk, B. Pozsgay, and M. B. Zvonarev, Finite temperature spin diffusion in the Hubbard model in the strong coupling limit, SciPost Phys. **15**, 073 (2023).
[62] E. Tartaglia, P. Calabrese, and B. Bertini, Real-time evolution in the Hubbard model with infinite repulsion, SciPost Phys. **12**, 028 (2022).
[63] B. Pozsgay, T. Gombor, A. Hutsalyuk, Y. Jiang, L. Pristyák, and E. Vernier, Integrable spin chain with Hilbert space fragmentation and solvable real-time dynamics, Phys. Rev. E **104**, 044106 (2021).
[64] J. Feldmeier, W. Witczak-Krempa, and M. Knap, Emergent tracer dynamics in constrained quantum systems, Phys. Rev. B **106**, 094303 (2022).
[65] M. Borsi, L. Pristyák, and B. Pozsgay, Matrix product symmetries and breakdown of thermalization from hard rod deformations, Phys. Rev. Lett. **131**, 037101 (2023).

[66] J.-J. Luo, S. Basak, H. Pu, and X.-W. Guan, Quantum transport in the one-dimensional Hubbard model: Drude weights and Seebeck effect, Phys. Rev. B **112**, 235414 (2025).
[67] P. Horsch and W. Stephan, Frequency-dependent conductivity of the one-dimensional Hubbard model at strong coupling, Phys. Rev. B **48**, 10595 (1993).
[68] K. Fujimoto, T. Ishiyama, T. Kurose, T. Yoshimura, and T. Sasamoto, Exact anomalous current fluctuations in quantum many-body dynamics, arXiv:2602.24008.
[69] J. M. P. Carmelo, S. Nemati, and T. Prosen, Absence of ballistic charge transport in the half-filled 1D Hubbard model, Nucl. Phys. **B930**, 418 (2018).
[70] J. M. P. Carmelo, S.-J. Gu, and P. Sacramento, Zero finite-temperature charge stiffness within the half-filled 1D Hubbard model, Ann. Phys. (Amsterdam) **339**, 484 (2013).
[71] P. Prelovšek, S. Elshawish, X. Zotos, and M. Long, Anomalous scaling of conductivity in integrable fermion systems, Phys. Rev. B **70**, 205129 (2004).
[72] C. Karrasch, D. M. Kennes, and J. E. Moore, Transport properties of the one-dimensional Hubbard model at finite temperature, Phys. Rev. B **90**, 155104 (2014).
[73] B. S. Shastry and B. Sutherland, Twisted boundary conditions and effective mass in Heisenberg-Ising and Hubbard rings, Phys. Rev. Lett. **65**, 243 (1990).
[74] C. A. Stafford, A. J. Millis, and B. S. Shastry, Finite-size effects on the optical conductivity of a half-filled Hubbard ring, Phys. Rev. B **43**, 13660 (1991).
[75] E. Ilievski and J. De Nardis, Ballistic transport in the one-dimensional Hubbard model: The hydrodynamic approach, Phys. Rev. B **96**, 081118(R) (2017).
[76] E. Ilievski, J. De Nardis, M. Medenjak, and T. Prosen, Superdiffusion in one-dimensional quantum lattice models, Phys. Rev. Lett. **121**, 230602 (2018).
[77] M. Fava, B. Ware, S. Gopalakrishnan, R. Vasseur, and S. A. Parameswaran, Spin crossovers and superdiffusion in the one-dimensional Hubbard model, Phys. Rev. B **102**, 115121 (2020).
[78] X. Zotos, F. Naef, and P. Prelovsek, Transport and conservation laws, Phys. Rev. B **55**, 11029 (1997).
[79] M. Garst and A. Rosch, Transport in a classical model of a one-dimensional Mott insulator: Influence of conservation laws, Europhys. Lett. **55**, 66 (2001).
[80] N. M. R. Peres, R. G. Dias, P. D. Sacramento, and J. M. P. Carmelo, Finite-temperature transport in finite-size Hubbard rings in the strong-coupling limit, Phys. Rev. B **61**, 5169 (2000).
[81] S. Fujimoto and N. Kawakami, Exact Drude weight for the one-dimensional Hubbard model at finite temperatures, J. Phys. A **31**, 465 (1998).
[82] W. Stephan and P. Horsch, Optical properties of one- and two-dimensional Hubbard and t-J models, Phys. Rev. B **42**, 8736 (1990).
[83] R. M. Fye, M. J. Martins, D. J. Scalapino, J. Wagner, and W. Hanke, Drude weight, optical conductivity, and flux properties of one-dimensional Hubbard rings, Phys. Rev. B **44**, 6909 (1991).
[84] F. Jin, R. Steinigeweg, F. Heidrich-Meisner, K. Michielsen, and H. De Raedt, Finite-temperature charge transport in the one-dimensional Hubbard model, Phys. Rev. B **92**, 205103 (2015).
[85] E. Jeckelmann, F. Gebhard, and F. H. L. Essler, Optical conductivity of the half-filled Hubbard chain, Phys. Rev. Lett. **85**, 3910 (2000).
[86] M. Aichhorn, M. Daghofer, H. G. Evertz, and W. von der Linden, Low-temperature Lanczos method for strongly correlated systems, Phys. Rev. B **67**, 161103(R) (2003).
[87] S. Kirchner, H. G. Evertz, and W. Hanke, Transport properties of one-dimensional Hubbard models, Phys. Rev. B **59**, 1825 (1999).
[88] See Supplemental Material at http://link.aps.org/supplemental/10.1103/2fwz-cw5h for (I) a linear-response derivation of the optical conductivity, (II) definitions of the model and observables, (III) the explicit eigenstates and energy spectrum, (IV) and (V) analytical expressions for the Drude weight, and (VI) an analysis of the effective resistivity, which includes Refs. [89–99].
[89] R. Kubo, Statistical-mechanical theory of irreversible processes. I. General theory and simple applications to magnetic and conduction problems, J. Phys. Soc. Jpn. **12**, 570 (1957).
[90] R. Peierls, Zur Theorie des Diamagnetismus von Leitungselektronen, Z. Phys. **80**, 763 (1933).
[91] D. N. Basov, R. D. Averitt, D. van der Marel, M. Dressel, and K. Haule, Electrodynamics of correlated electron materials, Rev. Mod. Phys. **83**, 471 (2011).
[92] A. Kuzmenko, Kramers–Kronig constrained variational analysis of optical spectra, Rev. Sci. Instrum. **76**, 083108 (2005).
[93] D. L. Colton and R. Kress, *Inverse Acoustic and Electromagnetic Scattering Theory* (Springer, New York, 1998), Vol. 93.
[94] A. A. Cuyt, V. Petersen, B. Verdonk, H. Waadeland, and W. B. Jones, *Handbook of Continued Fractions for Special Functions* (Springer Science & Business Media, New York, 2008).
[95] G. E. Andrews, *The Theory of Partitions* (Cambridge University Press, Cambridge, England, 1998), 2.
[96] T. M. Apostol, *Modular Functions and Dirichlet Series in Number Theory* (Springer Science & Business Media, New York, 2012).
[97] S. Mukerjee, V. Oganesyan, and D. Huse, Statistical theory of transport by strongly interacting lattice fermions, Phys. Rev. B **73**, 035113 (2006).
[98] S. Liu, A. Kumar, Y. Ma, P. W. Phillips, H. J. Changlani, and B. A. Bernevig, Energy-resolved current response and two regimes of approximately linear-in-T resistivity in the infinite-U Hubbard model (to be published).
[99] A. A. Patel and H. J. Changlani, Many-body energy invariant for T-linear resistivity, Phys. Rev. B **105**, L201108 (2022).
[100] X. Deng, J. Mravlje, R. Žitko, M. Ferrero, G. Kotliar, and A. Georges, How bad metals turn good: Spectroscopic signatures of resilient quasiparticles, Phys. Rev. Lett. **110**, 086401 (2013).
[101] N. Pakhira and R. H. McKenzie, Absence of a quantum limit to charge diffusion in bad metals, Phys. Rev. B **91**, 075124 (2015).

[102] J. Kokalj, Bad-metallic behavior of doped Mott insulators, Phys. Rev. B **95**, 041110(R) (2017).
[103] J. Vučičević, J. Kokalj, R. Žitko, N. Wentzell, D. Tanasković, and J. Mravlje, Conductivity in the square lattice Hubbard model at high temperatures: Importance of vertex corrections, Phys. Rev. Lett. **123**, 036601 (2019).
[104] E. W. Huang, R. Sheppard, B. Moritz, and T. P. Devereaux, Strange metallicity in the doped Hubbard model, Science **366**, 987 (2019).
[105] P. W. Phillips, N. E. Hussey, and P. Abbamonte, Stranger than metals, Science **377**, eabh4273 (2022).
[106] D. v. d. Marel, H. J. A. Molegraaf, J. Zaanen, Z. Nussinov, F. Carbone, A. Damascelli, H. Eisaki, M. Greven, P. H. Kes, and M. Li, Quantum critical behaviour in a high-Tc superconductor, Nature (London) **425**, 271 (2003).
[107] P. Fournier, P. Mohanty, E. Maiser, S. Darzens, T. Venkatesan, C. J. Lobb, G. Czjzek, R. A. Webb, and R. L. Greene, Insulator-metal crossover near optimal doping in $Pr_{2-x}Ce_xCuO_4$: Anomalous normal-state low temperature resistivity, Phys. Rev. Lett. **81**, 4720 (1998).
[108] Y. Dagan, M. M. Qazilbash, C. P. Hill, V. N. Kulkarni, and R. L. Greene, Evidence for a quantum phase transition in $Pr_{2-x}Ce_xCuO_{4-\delta}$ from transport measurements, Phys. Rev. Lett. **92**, 167001 (2004).
[109] K. Jin, N. P. Butch, K. Kirshenbaum, J. Paglione, and R. L. Greene, Link between spin fluctuations and electron pairing in copper oxide superconductors, Nature (London) **476**, 73 (2011).
[110] S. Martin, A. T. Fiory, R. M. Fleming, L. F. Schneemeyer, and J. V. Waszczak, Normal-state transport properties of $Bi_{2+x}Sr_{2-y}CuO_{6+\delta}$ crystals, Phys. Rev. B **41**, 846 (1990).
[111] R. A. Cooper, Y. Wang, B. Vignolle, O. J. Lipscombe, S. M. Hayden, Y. Tanabe, T. Adachi, Y. Koike, M. Nohara, H. Takagi, C. Proust, and N. E. Hussey, Anomalous criticality in the electrical resistivity of $La_{2-x}Sr_xCuO_4$, Science **323**, 603 (2009).
[112] R. Daou, N. Doiron-Leyraud, D. LeBoeuf, S. Y. Li, F. Laliberté, O. Cyr-Choinière, Y. J. Jo, L. Balicas, J.-Q. Yan, J.-S. Zhou, J. B. Goodenough, and L. Taillefer, Linear temperature dependence of resistivity and change in the Fermi surface at the pseudogap critical point of a high-Tc superconductor, Nat. Phys. **5**, 31 (2009).
[113] C. Collignon, S. Badoux, S. A. A. Afshar, B. Michon, F. Laliberté, O. Cyr-Choinière, J.-S. Zhou, S. Licciardello, S. Wiedmann, N. Doiron-Leyraud, and L. Taillefer, Fermi-surface transformation across the pseudogap critical point of the cuprate superconductor $La_{1.6-x}Nd_{0.4}Sr_xCuO_4$, Phys. Rev. B **95**, 224517 (2017).
[114] N. Doiron-Leyraud, O. Cyr-Choinière, S. Badoux, A. Ataei, C. Collignon, A. Gourgout, S. Dufour-Beaus'eour, F. F. Tafti, F. Laliberté, M.-E. Boulanger, M. Matusiak, D. Graf, M. Kim, J.-S. Zhou, N. Momono, T. Kurosawa, H. Takagi, and L. Taillefer, Pseudogap phase of cuprate superconductors confined by Fermi surface topology, Nat. Commun. **8**, 2044 (2017).
[115] A. Legros, S. Benhabib, W. Tabis, F. Laliberté, M. Dion, M. Lizaire, B. Vignolle, D. Vignolles, H. Raffy, Z. Z. Li, P. Auban-Senzier, N. Doiron-Leyraud, P. Fournier, D. Colson, L. Taillefer, and C. Proust, Universal T-linear resistivity and Planckian dissipation in overdoped cuprates, Nat. Phys. **15**, 142 (2019).
[116] P. T. Brown, D. Mitra, E. Guardado-Sanchez, R. Nourafkan, A. Reymbaut, C.-D. Hébert, S. Bergeron, A.-M. S. Tremblay, J. Kokalj, D. A. Huse, P. Schauß, and W. S. Bakr, Bad metallic transport in a cold atom Fermi-Hubbard system, Science **363**, 379 (2019).
[117] D. Chowdhury, A. Georges, O. Parcollet, and S. Sachdev, Sachdev-Ye-Kitaev models and beyond: Window into non-Fermi liquids, Rev. Mod. Phys. **94**, 035004 (2022).
[118] A. A. Patel, H. Guo, I. Esterlis, and S. Sachdev, Universal theory of strange metals from spatially random interactions, Science **381**, 790 (2023).
[119] P. Cha, N. Wentzell, O. Parcollet, A. Georges, and E.-A. Kim, Linear resistivity and Sachdev-Ye-Kitaev (SYK) spin liquid behavior in a quantum critical metal with spin-1/2 fermions, Proc. Natl. Acad. Sci. U.S.A. **117**, 18341 (2020).
[120] C. Li, D. Valentinis, A. A. Patel, H. Guo, J. Schmalian, S. Sachdev, and I. Esterlis, Strange metal and superconductor in the two-dimensional Yukawa-Sachdev-Ye-Kitaev model, Phys. Rev. Lett. **133**, 186502 (2024).
[121] H. Polshyn, M. Yankowitz, S. Chen, Y. Zhang, K. Watanabe, T. Taniguchi, C. R. Dean, and A. F. Young, Large linear-in-temperature resistivity in twisted bilayer graphene, Nat. Phys. **15**, 1011 (2019).
[122] F. Wu, E. Hwang, and S. Das Sarma, Phonon-induced giant linear-in-T resistivity in magic angle twisted bilayer graphene: Ordinary strangeness and exotic superconductivity, Phys. Rev. B **99**, 165112 (2019).
[123] Y. Cao, D. Chowdhury, D. Rodan-Legrain, O. Rubies-Bigorda, K. Watanabe, T. Taniguchi, T. Senthil, and P. Jarillo-Herrero, Strange metal in magic-angle graphene with near Planckian dissipation, Phys. Rev. Lett. **124**, 076801 (2020).
[124] A. Jaoui, I. Das, G. Di Battista, J. Díez-Mérida, X. Lu, K. Watanabe, T. Taniguchi, H. Ishizuka, L. Levitov, and D. K. Efetov, Quantum critical behaviour in magic-angle twisted bilayer graphene, Nat. Phys. **18**, 633 (2022).
[125] P. Mazur, Non-ergodicity of phase functions in certain systems, Physica (Amsterdam) **43**, 533 (1969).
[126] P. F. Maldague, Optical spectrum of a Hubbard chain, Phys. Rev. B **16**, 2437 (1977).
[127] D. Baeriswyl, C. Gros, and T. M. Rice, Landau parameters of almost-localized Fermi liquids, Phys. Rev. B **35**, 8391 (1987).
[128] D. J. Scalapino, S. R. White, and S. C. Zhang, Superfluid density and the Drude weight of the Hubbard model, Phys. Rev. Lett. **68**, 2830 (1992).
[129] A. Abouelkomsan, N. Paul, A. Stern, and L. Fu, Compressible quantum liquid with vanishing Drude weight, Phys. Rev. Lett. **134**, 176501 (2025).
[130] B. S. Shastry, Sum rule for thermal conductivity and dynamical thermal transport coefficients in condensed matter, Phys. Rev. B **73**, 085117 (2006).
[131] S. Mukerjee and B. S. Shastry, Signatures of diffusion and ballistic transport in the stiffness, dynamical correlation functions, and statistics of one-dimensional systems, Phys. Rev. B **77**, 245131 (2008).

[132] H. J. Schulz, Correlation exponents and the metal-insulator transition in the one-dimensional Hubbard model, Phys. Rev. Lett. **64**, 2831 (1990).

[133] A. Moreno, A. Muramatsu, and S. R. Manmana, Ground-state phase diagram of the one-dimensional *t-J* model, Phys. Rev. B **83**, 205113 (2011).

[134] Y.-F. Song, Y. Deng, and Y.-Y. He, Magnetic, thermodynamic, and dynamical properties of the three-dimensional fermionic Hubbard model: A comprehensive Monte Carlo study, Phys. Rev. B **111**, 035123 (2025).

[135] M. Lu, Y.-F. Song, Y. Deng, and Y.-Y. He, Quantum Monte Carlo study of the metal-insulator crossover in the square-lattice Hubbard model, Phys. Rev. B **113**, 195154 (2026).

[136] S. Liu, H. J. Changlani, and B. A. Bernevig (to be published).

[137] P. Mai, J. Zhao, G. Tenkila, N. A. Hackner, D. Kush, D. Pan, and P. W. Phillips, Twisting the Hubbard model into the momentum-mixing Hatsugai–Kohmoto model, Nat. Phys. **22**, 81 (2026).

[138] Y. Ma, J. Zhao, E. W. Huang, D. Kush, B. Bradlyn, and P. W. Phillips, Charge susceptibility and Kubo response in Hatsugai-Kohmoto-related models, Phys. Rev. B **112**, 045109 (2025).